Tidal stirring of disky dwarfs with shallow dark matter density profiles: Enhanced transformation into dwarf spheroidals

Kazantzidis, Stelios ; Łokas, Ewa L ; Mayer, Lucio

Abstract: According to the tidal stirring model, late type, rotationally supported dwarfs resembling present day dwarf irregular (dIrr) galaxies can transform into dwarf spheroidals (dSphs) via interactions with Milky-Way-sized hosts. We perform collisionless N-body simulations to investigate for the first time how tidal stirring depends on the dark matter (DM) density distribution in the central stellar region of the progenitor disky dwarf. Specifically, we explore various asymptotic inner slopes of the dwarf DM density profiles (vpropr -). For a given orbit inside the primary galaxy, rotationally supported dwarfs embedded in DM halos with core-like distributions (= 0.2) and mild density cusps (= 0.6) demonstrate a substantially enhanced likelihood and efficiency of transformation into dSphs compared to their counterparts with steeper DM density profiles (= 1). Such shallow DM distributions are akin to those of observed dIrrs highlighting tidal stirring as a plausible model for the Local Group (LG) morphology-density relation. When < 1, a single pericentric passage can induce dSph formation and disky dwarfs on low-eccentricity or large-pericenter orbits are able to transform; these new results allow tidal stirring to explain virtually all known dSphs across a wide range of distances from their hosts. A subset of disky dwarfs initially embedded in DM halos with shallow density profiles are eventually disrupted by the primary; those that survive as dSphs are generally on orbits with lower eccentricities and/or larger pericenters compared to those of typical cold dark matter satellites. The latter could explain the peculiar orbits of several LG dSphs such as Fornax, Leo I, Tucana, and Cetus.

DOI: https://doi.org/10.1088/2041-8205/764/2/L29

The Astrophysical Journal Letters, 764:L29 (6pp), 2013 February 20 doi:10.1088/2041-8205/764/2/L29

TIDAL STIRRING OF DISKY DWARFS WITH SHALLOW DARK MATTER DENSITY PROFILES: ENHANCED TRANSFORMATION INTO DWARF SPHEROIDALS

Stelios Kazantzidis[1,2,3], Ewa L. Łokas[4], and Lucio Mayer[5]
[1] Center for Cosmology and Astro-Particle Physics, The Ohio State University, Columbus, OH 43210, USA; stelios@mps.ohio-state.edu
[2] Department of Physics, The Ohio State University, Columbus, OH 43210, USA
[3] Department of Astronomy, The Ohio State University, Columbus, OH 43210, USA
[4] Nicolaus Copernicus Astronomical Center, 00-716 Warsaw, Poland
[5] Institute for Theoretical Physics, University of Zürich, CH-8057 Zürich, Switzerland
Received 2012 November 17; accepted 2013 January 26; published 2013 February 7

ABSTRACT

According to the tidal stirring model, late type, rotationally supported dwarfs resembling present day dwarf irregular (dIrr) galaxies can transform into dwarf spheroidals (dSphs) via interactions with Milky-Way-sized hosts. We perform collisionless *N*-body simulations to investigate for the first time how tidal stirring depends on the dark matter (DM) density distribution in the central stellar region of the progenitor disky dwarf. Specifically, we explore various asymptotic inner slopes γ of the dwarf DM density profiles ($\rho \propto r^{-\gamma}$). For a given orbit inside the primary galaxy, rotationally supported dwarfs embedded in DM halos with core-like distributions ($\gamma = 0.2$) and mild density cusps ($\gamma = 0.6$) demonstrate a substantially enhanced likelihood and efficiency of transformation into dSphs compared to their counterparts with steeper DM density profiles ($\gamma = 1$). Such shallow DM distributions are akin to those of observed dIrrs highlighting tidal stirring as a plausible model for the Local Group (LG) morphology–density relation. When $\gamma < 1$, a single pericentric passage can induce dSph formation and disky dwarfs on low-eccentricity or large-pericenter orbits are able to transform; these new results allow tidal stirring to explain virtually all known dSphs across a wide range of distances from their hosts. A subset of disky dwarfs initially embedded in DM halos with shallow density profiles are eventually disrupted by the primary; those that survive as dSphs are generally on orbits with lower eccentricities and/or larger pericenters compared to those of typical cold dark matter satellites. The latter could explain the peculiar orbits of several LG dSphs such as Fornax, Leo I, Tucana, and Cetus.

Key words: galaxies: dwarf – galaxies: formation – galaxies: kinematics and dynamics – galaxies: structure – Local Group – methods: numerical

Online-only material: color figures

1. INTRODUCTION

The dwarf spheroidal (dSph) satellites in the Local Group (LG) are the faintest and most dark matter (DM) dominated galaxies known (e.g., Mateo 1998; Tolstoy et al. 2009). These intriguing objects exhibit no appreciable gas components (e.g., Grcevich & Putman 2009) and are typically clustered around the dominant spiral galaxies Milky Way (MW) and M31. Despite recent advances in our understanding of dSphs, a conclusive model for their origin has yet to emerge (e.g., Kravtsov 2010).

Various environmental processes have been invoked to explain the formation of dSphs, including tidal and ram pressure stripping (e.g., Einasto et al. 1974; Faber & Lin 1983; Mayer et al. 2001, 2006, 2007; Kravtsov et al. 2004; Klimentowski et al. 2009; Kazantzidis et al. 2011a; Łokas et al. 2011), mergers between dwarfs (Kazantzidis et al. 2011b; Yozin & Bekki 2012), and resonant stripping (D'Onghia et al. 2009). In this context, the "tidal stirring" model (Mayer et al. 2001) posits that interactions with MW-sized host galaxies can transform late-type dwarfs resembling present-day dwarf irregular galaxies (dIrrs) into dSphs.

Earlier tidal stirring studies have almost exclusively adopted cuspy, Navarro et al. (1996, hereafter NFW) density profiles to model the DM halos of the progenitor disky dwarfs. Yet, rotation-curve modeling of observed dIrrs (e.g., Weldrake et al. 2003; Oh et al. 2011), which constitute the most plausible dSph progenitors according to tidal stirring, favors DM halos with significantly shallower inner density slopes. Such shallow density distributions are also supported by hydrodynamical cosmological simulations of dwarf galaxy formation (Governato et al. 2010) and recent analytic models for the origin of core-like DM density profiles in dwarfs (Pontzen & Governato 2012).

The cuspiness of the dwarf DM distribution in the central region where the stars reside should play a crucial role in tidal stirring. Indeed, rotationally supported dwarfs with shallow DM density profiles are characterized by lower central densities and, correspondingly, longer internal dynamical times compared to their counterparts with steeper DM density distributions. Systems with longer dynamical times respond more impulsively to external tidal perturbations and suffer stronger tidal heating (e.g., Gnedin & Ostriker 1999). Disky dwarfs with progressively shallower DM density profiles may thus experience increasingly probable and efficient transformations into dSphs. Nonetheless, there has been no *quantitative* work aimed at investigating this qualitative expectation. Here we investigate this issue via a series of tidal stirring simulations of rotationally supported dwarfs embedded in DM halos with different inner density distributions.

2. METHODS

A description of the adopted methodology is given in Łokas et al. (2012). We employed the method of Widrow et al. (2008) to construct numerical realizations of dwarf galaxies consisting of exponential stellar disks embedded in DM halos. The DM halo density profiles followed the form (Łokas 2002),

$$\rho(r) = \frac{\rho_s}{(r/r_s)^{\gamma}(1 + r/r_s)^{3-\gamma}}, \quad (1)$$

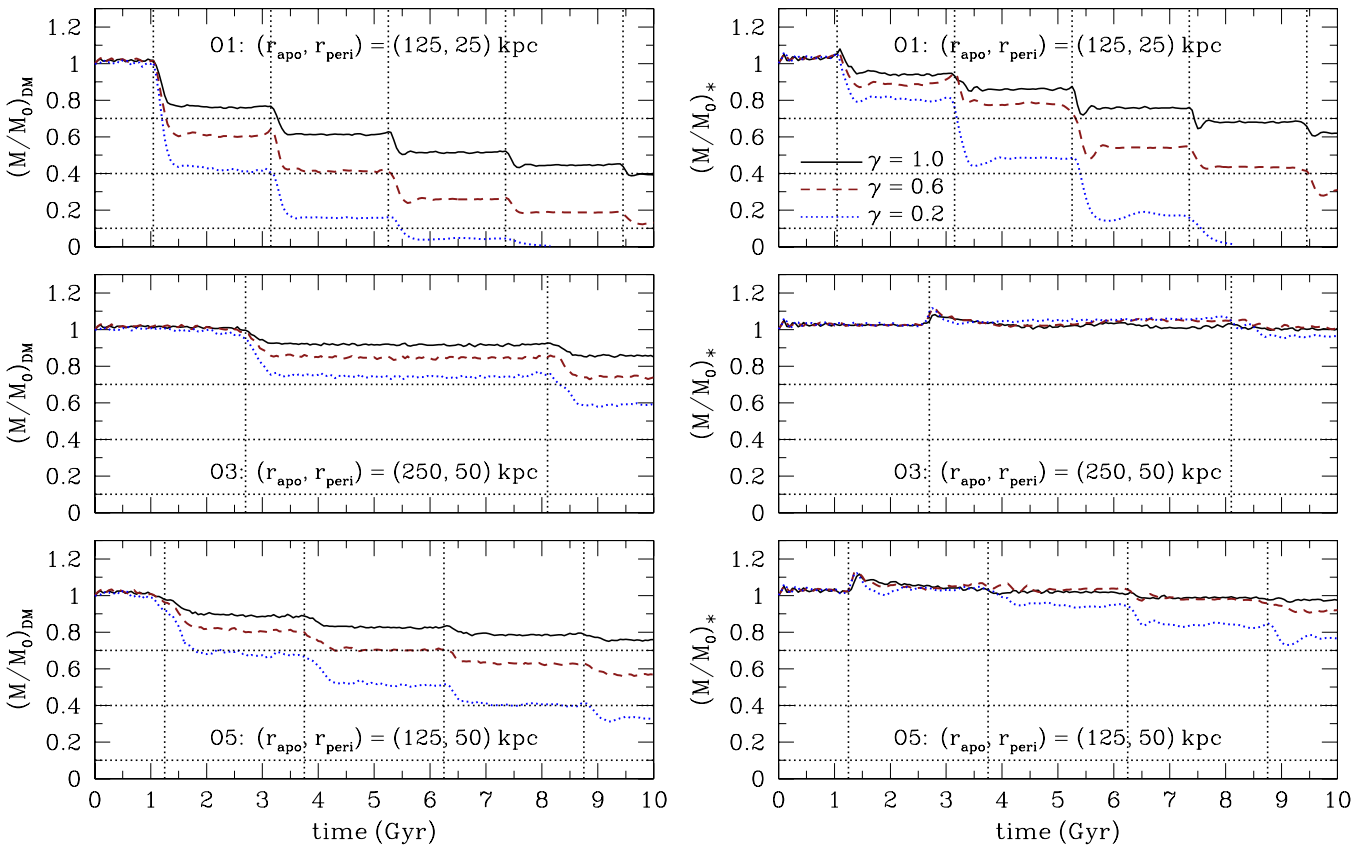

Figure 1. Evolution of mass in the DM (left panels) and stellar (right panels) components of the simulated disky dwarfs as a function of time. The results are presented for orbits O1 (upper panels), O3 (middle panels), and O5 (lower panels). DM (stellar) masses are computed within 0.7 kpc from the center of the dwarf (see the text) and are normalized to the *initial* DM (stellar) mass enclosed within 0.7 kpc, M_0. The vertical lines specify pericentric passages and horizontal lines indicate mass loss of 30%, 60%, and 90% with respect to the initial value. For a given orbit inside the host, rotationally supported dwarfs embedded in DM halos with shallow density profiles ($\gamma < 1$) experience enhanced mass loss compared to their counterparts with steeper DM density distributions ($\gamma = 1$).

(A color version of this figure is available in the online journal.)

where ρ_s, r_s, and γ denote the characteristic inner density, the scale radius, and the *asymptotic* inner slope of the profile, respectively. ρ_s depends on the epoch of halo formation, the present-day values of the cosmological parameters, and γ (throughout the Letter we assume the concordance ΛCDM cosmogony and $z = 0$).

To examine how the DM density distribution in the central stellar region of the progenitor disky dwarf affects tidal stirring, we varied γ in three otherwise identically initialized dwarf galaxies. Specifically, we adopted $\gamma = 1$ (corresponding to the NFW profile) and two shallower inner slopes, namely, a mild density cusp ($\gamma = 0.6$) and a nearly constant density core ($\gamma = 0.2$). These shallow slopes are well motivated as they are akin to those of both observed dIrrs (e.g., Weldrake et al. 2003; Oh et al. 2011) and realistic dIrr-like systems formed in hydrodynamical cosmological simulations (Governato et al. 2010).

Each dwarf galaxy comprised a DM halo with a virial mass of $M_{\rm vir} = 10^9\,M_\odot$ (virial radius of $r_{\rm vir} \approx 25.9$ kpc) and a concentration parameter of $c \equiv r_{\rm vir}/r_s = 20$ ($r_s \approx 1.29$ kpc), and was exponentially truncated beyond $r_{\rm vir}$ (Kazantzidis et al. 2004a). All DM halos hosted an identical stellar disk whose mass, radial scale length, sech^2 vertical scale height, and central radial velocity dispersion were equal to $M_d = 0.02\,M_{\rm vir}$, $R_d \approx 0.41$ kpc, $z_d = 0.2\,R_d$, and $\sigma_{R0} = 10\,{\rm km\,s^{-1}}$, respectively. The value of R_d is derived assuming a halo spin parameter of $\lambda = 0.04$ (Mo et al. 1998). Being embedded in different DM density distributions, the resulting disks differed in their velocity dispersion profile and Toomre Q stability parameter. All dwarfs were stable against bar formation in isolation.

Our choices of γ lead to DM density profiles, circular velocity profiles, and stellar binding energy distributions that display substantially dissimilar shapes within $5\,R_d \approx 2$ kpc, namely, the radius containing the vast majority (>95%) of disk stars (see Figure 1 of Łokas et al. 2012). Hence, although our modeling approach is certainly not unique, it does serve our purpose by ensuring that the employed rotationally supported dwarfs exhibit markedly different initial properties in the central stellar region. Specifically, decreasing cusp slopes result in less concentrated mass and energy distributions, less steeply rising circular velocity profiles, and smaller maximum circular velocities $V_{\rm max}$ (the $V_{\rm max}$ differ by $\approx$3 km s^{-1} between $\gamma = 1$ and $\gamma = 0.2$). Therefore, disky dwarfs embedded in DM halos with shallow density profiles are expected to manifest significantly different responses to tidal shocks and overall tidal evolutions compared to their counterparts with steeper DM density distributions. We shall quantify these differences in the following section.

We used $N_h = 10^6$ DM and $N_d = 5 \times 10^5$ disk particles to realize the dwarf models and set the gravitational softening to $\epsilon_h = 60$ pc and $\epsilon_d = 20$ pc, respectively. We assumed a single host represented by a self-gravitating numerical model of the MW (Kazantzidis et al. 2011a). Each disky dwarf was placed on five different orbits inside the host, whose parameters were motivated by both theoretical studies of the orbital distributions of cosmological halos in MW-sized hosts

Table 1
Orbital Parameters of Disky Dwarfs

Orbit	$r_{\rm apo}$ (kpc)	$r_{\rm apo}/r_{\rm peri}$	$r_{\rm peri}$ (kpc)	$T_{\rm orb}$ (Gyr)
(1)	(2)	(3)	(4)	(5)
O1	125	5	25	2.1
O2	85	5	17	1.3
O3	250	5	50	5.4
O4	125	10	12.5	1.8
O5	125	2.5	50	2.5

(e.g., Diemand et al. 2007; Klimentowski et al. 2010) and observational work pertaining to LG dwarfs (e.g., McConnachie 2012). Table 1 summarizes the adopted orbital parameters, including apocentric distances, $r_{\rm apo}$, eccentricities, $r_{\rm apo}/r_{\rm peri}$, pericentric distances, $r_{\rm peri}$, and orbital times, $T_{\rm orb}$. In all cases, the dwarfs started at apocenter and were evolved for 10 Gyr inside the primary. The alignments between the internal angular momenta of the dwarfs, those of the primary disks and the orbital angular momenta were all always prograde and equal to 45° (Kazantzidis et al. 2011a). The simulations were performed with the *N*-body code PKDGRAV (Stadel 2001).

3. RESULTS

We examined the global response of our disky dwarfs subject to the host tidal field via the evolution of their masses, kinematics, and shapes. These properties were always computed within 0.7 kpc from the dwarf center, a radius that is approximately equal to the half-light radius, $r_{1/2}$, of the initial disk. Adopting this well-defined, fixed scale facilitates meaningful comparisons among different experiments and enables us to overcome the complications associated with determining tidal radii (e.g., Read et al. 2006).

We quantified the dwarf kinematics and shapes through the parameters $V_{\rm rot}/\sigma_*$ and c/a, where $V_{\rm rot}$, σ_*, c, and a denote the rotational velocity, the one-dimensional velocity dispersion, the minor axis, and the major axis of the stellar distribution, respectively. At each simulation output, the following procedure was repeated. We first determined the directions of the principal axes and derived c/a using the moments of the inertia tensor. Subsequently, we introduced a spherical coordinate system (r, θ, ϕ), where ϕ is the angle coordinate in the xy plane oriented in such a way that the z-axis is along the minor axis of the stellar distribution. We calculated $V_{\rm rot}$ around the minor axis $V_{\rm rot} = V_\phi$ and defined $\sigma_* \equiv [(\sigma_r^2 + \sigma_\theta^2 + \sigma_\phi^2)/3]^{1/2}$.

Given the typical parameters associated with orbit O1, we use it as the basis for the comparison with the other experiments. In what follows, we only describe results pertaining to orbits O1, O3, and O5. This is for brevity and because the evolution of the rotationally supported dwarfs on the tightest (O2) and the most eccentric (O4) orbits displays similar salient features to those of O1. We stress that orbits O3 and O5 are characterized by larger pericenters and/or lower eccentricities compared to those of representative cold dark matter (CDM) satellites (e.g., Diemand et al. 2007).

Figure 1 shows the time evolution of the DM and stellar masses of the disky dwarfs as they orbit inside the primary. Masses decrease significantly at the pericenters of the orbit, where the tidal shocks occur. Between pericentric passages, masses remain remarkably constant, indicating that the dwarfs respond nearly adiabatically to the tidal field. Irrespective of orbit, disky dwarfs embedded in DM halos with shallow density profiles ($\gamma < 1$) suffer augmented mass loss in both stellar and DM components compared to their counterparts with steeper DM density distributions (Kazantzidis et al. 2004b; Peñarrubia et al. 2010). In some circumstances, the amount of mass loss is so dramatic that it leads to complete tidal disruption. Columns 4 and 5 of Table 2 provide information regarding dwarf survival (as indicated by the presence of a self-bound entity at $t = 10$ Gyr) and list the time of disruption if it occurs, respectively.

Figure 2 presents the time evolution of $V_{\rm rot}/\sigma_*$ and c/a of the simulated disky dwarfs as they orbit inside the host galaxy. Given that $V_{\rm rot}$ is larger for more concentrated mass distributions and that all dwarf models are initialized with the same σ_{R0}, steeper cusp slopes result in greater initial values of $V_{\rm rot}/\sigma_*$. Injection of energy via tidal shocks at pericentric passages increases the random motions of disk stars, causing their orbits to become more isotropic. Hence, $V_{\rm rot}/\sigma_*$ progressively decreases, signifying the transition from rotationally supported to pressure-supported stellar systems. Simultaneously, the initially disky stellar distributions evolve into more spheroidal shapes as reflected in the continuous increase of c/a. Figure 2 demonstrates that, regardless of orbit, rotationally supported dwarfs embedded in DM halos with shallow density profiles ($\gamma < 1$) exhibit stronger evolution in their kinematics and shapes compared to their counterparts with steeper DM density distributions ($\gamma = 1$).

We note that the strong tidal forces at pericenters typically trigger bar instabilities in the dwarf disks. These tidally induced bars play a vital role in the overall decrease of $V_{\rm rot}$ by transporting angular momentum outward. As tidal stripping removes the dwarf outer parts, the entire angular momentum content gradually decreases and the ability of the dwarf galaxy to be supported by rotation progressively diminishes. The seemingly unexpected increase of $V_{\rm rot}/\sigma_*$ between some pericentric passages is due to the particular orientation of these bars at the moment of pericenter crossing and the strong tidal torques exerted on them by the primary galaxy, resulting in an increase of $V_{\rm rot}$; Kazantzidis et al. 2011a). Column 6 of Table 2 indicates that bar formation is more probable in shallow DM density distributions (Mayer & Wadsley 2004).

Our primary goal is to assess the likelihood and efficiency of transformation into a dSph via tidal stirring. In accordance with observational studies of LG dwarfs (e.g., Mateo 1998; McConnachie 2012), we classify as *bona fide* dSphs in our simulations only those systems whose final states are characterized by $V_{\rm rot}/\sigma_* \lesssim 0.5$ and $c/a \gtrsim 0.5$. We stress that the criterion $V_{\rm rot}/\sigma_* \lesssim 0.5$ for establishing dSph formation should be regarded as fairly conservative. Indeed, we measure $V_{\rm rot}$ around the minor axis of the stellar distribution, which corresponds to observing the simulated dwarfs perfectly edge-on. Consequently, $V_{\rm rot}$ is *nearly* equivalent to the maximum rotational velocity and, thus, the values of $V_{\rm rot}/\sigma_*$ that we quote throughout the Letter are essentially the largest possible. Adopting a random line of sight would result in smaller $V_{\rm rot}/\sigma_*$ values, indicating even stronger and more complete transformations.

Columns 7 and 8 of Table 2 list the final values of $V_{\rm rot}/\sigma_*$ and c/a, respectively. These correspond to different timescales (from ∼4 to 10 Gyr) that are determined by the presence of a well-defined, bound stellar component of ∼0.7 kpc in size. Column 9 reports whether a dSph was produced according to the two criteria above. The notation "dSph?" in this column is introduced to account for observed dSphs that exhibit $0.5 \lesssim V_{\rm rot}/\sigma_* \lesssim 1$ such as Cetus (Lewis et al. 2007), Tucana (Fraternali et al. 2009), and Andromeda II (Ho et al. 2012). Of the disky

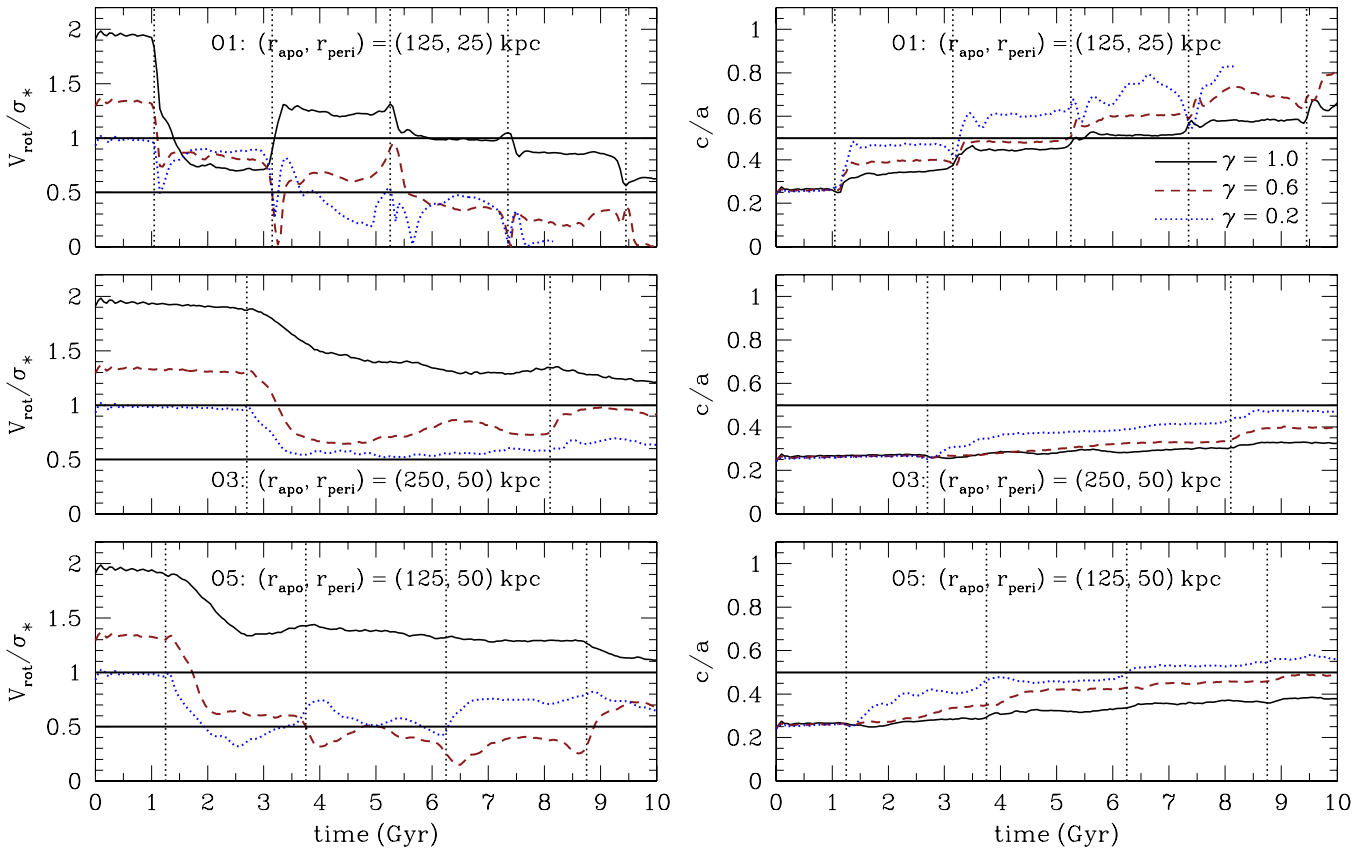

Figure 2. Evolution of stellar kinematics (left panels) and shape (right panels) of the simulated disky dwarfs as a function of time. The results are presented for orbits O1 (upper panels), O3 (middle panels), and O5 (lower panels). The line types are as in Figure 1. The horizontal lines indicate the limiting values $V_{\rm rot}/\sigma_* = 1$, $V_{\rm rot}/\sigma_* = 0.5$, and $c/a = 0.5$: simulated dwarf galaxies whose final states are characterized by $V_{\rm rot}/\sigma_* \lesssim 0.5$ and $c/a \gtrsim 0.5$ correspond to *bona fide* dSphs, while those with final values of $0.5 \lesssim V_{\rm rot}/\sigma_* \lesssim 1$ and $c/a \gtrsim 0.5$ are classified as "dSph?" (see the text). For a given orbit inside the host, rotationally supported dwarfs embedded in DM halos with shallow density profiles ($\gamma < 1$) experience a stronger evolution in their shapes and kinematics and demonstrate a considerably enhanced likelihood and efficiency of transformation into dSph-like systems relative to their counterparts with steeper DM density distributions ($\gamma = 1$).

(A color version of this figure is available in the online journal.)

Table 2
Summary of Results

Simulation	γ	Orbit	Survival	t_d (Gyr)	Bar Formation	$V_{\rm rot}/\sigma_*$	c/a	Classification	$t_{\rm dSph}$ (Gyr)
(1)	(2)	(3)	(4)	(5)	(6)	(7)	(8)	(9)	(10)
S1	1.0	O1	Yes	···	Yes	0.63	0.66	dSph?	···
S2	1.0	O2	Yes	···	Yes	0.01	0.93	dSph	2.85 (2)
S3	1.0	O3	Yes	···	No	1.21	0.33	Non-dSph	···
S4	1.0	O4	Yes	···	Yes	0.06	0.93	dSph	3.75 (2)
S5	1.0	O5	Yes	···	No	1.11	0.38	Non-dSph	···
S6	0.6	O1	Yes	···	Yes	0.01	0.82	dSph	5.55 (3)
S7	0.6	O2	No	6.40	Yes	0.01	0.82	dSph	2.55 (2)
S8	0.6	O3	Yes	···	No	0.92	0.40	Non-dSph	···
S9	0.6	O4	No	9.30	Yes	0.07	0.76	dSph	3.35 (2)
S10	0.6	O5	Yes	···	Yes	0.67	0.49	dSph?	···
S11	0.2	O1	No	8.15	Yes	0.06	0.83	dSph	3.70 (2)
S12	0.2	O2	No	3.80	Yes	0.07	0.82	dSph	1.85 (1)
S13	0.2	O3	Yes	···	Yes	0.63	0.47	dSph?	···
S14	0.2	O4	No	3.35	Yes	0.15	0.68	dSph	2.60 (1)
S15	0.2	O5	Yes	···	Yes	0.64	0.56	dSph?	···

dwarfs initially embedded in cuspy DM halos ($\gamma = 1$), only those on high-eccentricity ($r_{\rm apo}/r_{\rm peri} \gtrsim 5$) and small-pericenter ($r_{\rm peri} \lesssim 25$ kpc) orbits are transformed into objects with the properties of dSphs. Interestingly, the likelihood of dSph formation is enhanced significantly when $\gamma < 1$; in such cases, rotationally supported dwarfs on previously unfavorable low-eccentricity and/or large-pericenter orbits are able to transform into dSph-like systems. Figure 3 shows the surface density maps of the final stellar distributions of the dwarfs and visually confirms these conclusions.

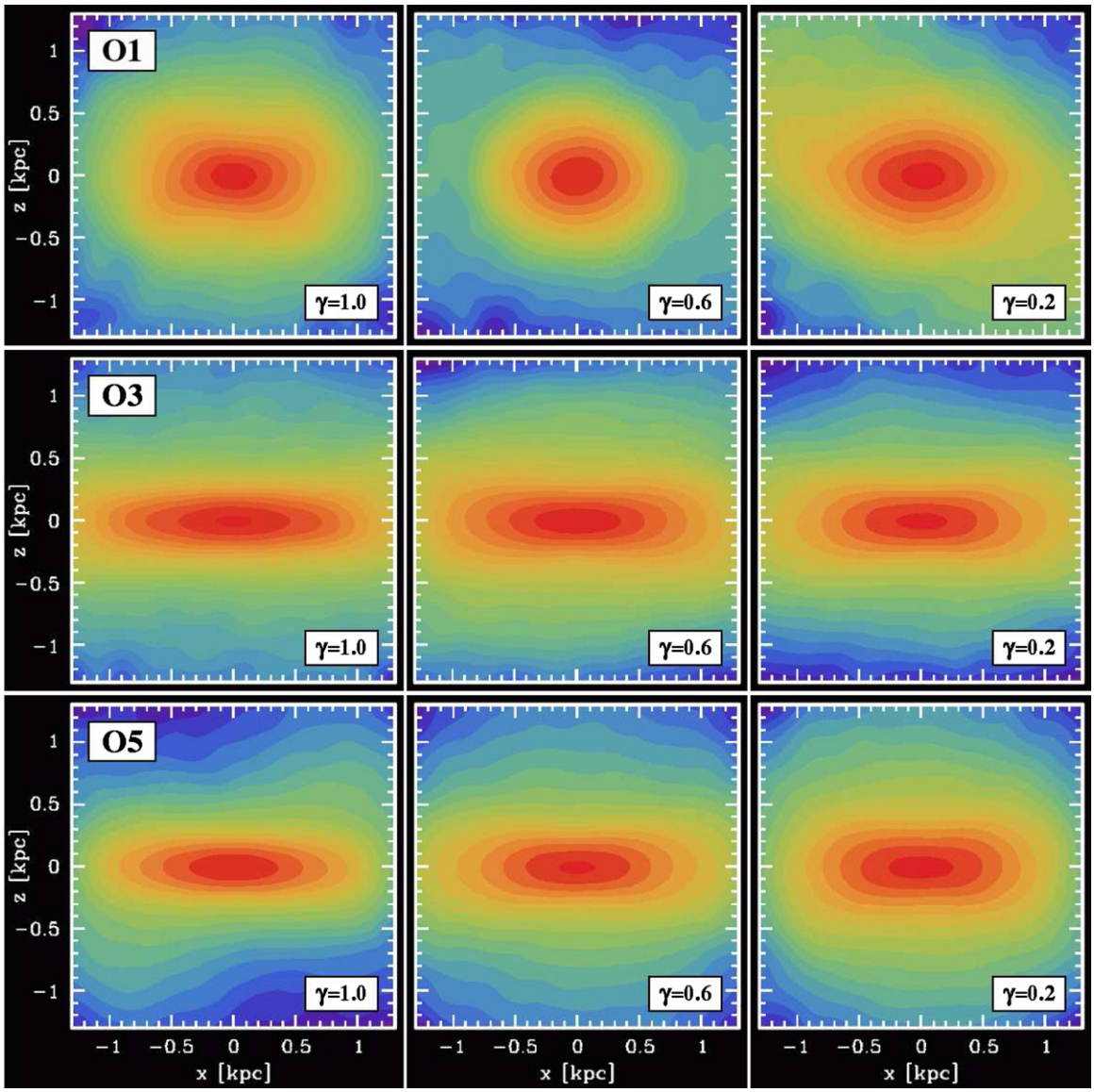

Figure 3. Surface number density distribution of stars in the simulated dwarfs. The results are presented for orbits O1 (upper panels), O3 (middle panels), and O5 (lower panels). All stellar components are depicted at $t = 10$ Gyr, except for that in the upper rightmost panel (O1; $\gamma = 0.2$) which is shown at $t = 6.35$ Gyr (corresponding to the timescale of the last apocenter before the disruption of the dwarf galaxy). The asymptotic inner slope of the dwarf DM density profile, γ, is indicated in each panel. The images show the most non-spherical views along the intermediate axis of the stellar distribution, y (where x and z denote the major and minor axes, respectively). The stars are binned into 0.2 kpc × 0.2 kpc fields perpendicular to the line of sight. The contours correspond to the number of stars N within each bin and are equally spaced by 0.2 in log N. The innermost contours are in the range log $N = 3.6$–4.6 depending on the case.

(A color version of this figure is available in the online journal.)

Inspection of Columns 6 and 9 of Table 2 illustrates that bar instabilities and dSph formation only occur in conjunction with one another, highlighting a strong association between bar formation and transformation into a dSph (e.g., Mayer et al. 2001; Klimentowski et al. 2009; Kazantzidis et al. 2011a). Column 10 of Table 2 lists the time elapsed from the beginning of the simulation until dSph formation occurs (the number of corresponding pericentric passages is included in parentheses) and shows that the efficiency of dSph formation is also substantially increased for shallow DM density profiles.

4. DISCUSSION

We have shown that, regardless of orbit inside the host, rotationally supported dwarfs embedded in DM halos with core-like distributions ($\gamma = 0.2$) and mild density cusps ($\gamma = 0.6$) demonstrate a considerably enhanced likelihood and efficiency of transformation into dSphs relative to their counterparts with NFW-like steeper DM density profiles ($\gamma = 1$). Such shallow DM distributions are akin to those inferred from the mass modeling of observed LG dIrrs (e.g., Weldrake et al. 2003) and analogous galaxies outside of the LG (e.g., Oh et al. 2011). Therefore, tidal stirring constitutes a plausible mechanism for explaining the origin of the LG morphology–density relation (e.g., Mateo 1998).

As shown in Łokas et al. (2012), the fractional increase in energy caused by the tidal shocks is given by $\Delta E/E \propto R^3/M$, where M denotes the dwarf mass within a characteristic radius R. At a given distance R from the center of our initial rotationally supported dwarf galaxies, decreasing cusp slopes correspond to smaller M, and thus to larger $\Delta E/E$. This explains why the $\gamma = 0.6$ and $\gamma = 0.2$ disky dwarfs experience stronger tidal shocks

and augmented mass loss relative to their $\gamma = 1$ counterparts, leading to their enhanced morphological transformation into dSphs. Considering adiabatic corrections to the energy change predicted by the impulse approximation (e.g., Gnedin & Ostriker 1999) would only reinforce this conclusion. Indeed, given that such corrections are inversely proportional to a power of the stellar orbital frequency ω and ω is higher at a given radius for more concentrated mass distributions, decreasing cusp slopes would correspond to even larger $\Delta E/E$ compared to those predicted by the impulse approximation.

The increased mass loss and rate of disruption experienced by dwarfs embedded in shallow DM halos have important implications for alleviating the missing satellites problem (Moore et al. 1999; Klypin et al. 1999). These findings also suggest that the dwarf luminosity and mass functions must be shifted lower relative to those of ΛCDM simulations that do not take into account baryonic effects (such as outflows triggered by supernovae explosions; see Governato et al. 2010) which can give rise to flattening of DM cusps. Consequently, claims regarding the agreement between theory and observations of the luminosity function and the radial distribution of satellites within MW-sized host halos (e.g., Macciò et al. 2010) may need revision.

The present study establishes tidal stirring as an even more prevalent transformation mechanism than previously considered. Earlier work adopting cuspy DM distributions for the progenitor disky dwarfs has indicated that only orbits characterized by high eccentricities ($r_{\rm apo}/r_{\rm peri} \gtrsim 5$), typical of CDM structure formation models (e.g., Diemand et al. 2007), and/or small pericentric distances ($r_{\rm peri} \lesssim 25$ kpc) are capable of transforming rotationally supported dwarfs into dSphs (e.g., Mayer et al. 2001; Kazantzidis et al. 2011a). For a transformation to occur, the same studies have also concluded that $T_{\rm orb}$ should be short enough to allow the progenitor disky dwarfs to complete at least two pericentric passages inside their hosts. These two requirements are probably not met for a number of LG dSphs, a fact that questioned the widespread applicability of tidal stirring.

For example, the distant dSphs Leo I, Cetus, and Tucana (residing in the LG outskirts at several hundred kpc from the MW and M31; e.g., Caputo et al. 1999; McConnachie et al. 2005; Saviane et al. 1996) are likely moving on very wide orbits associated with extremely long $T_{\rm orb}$. Moreover, proper-motion measurements have indicated a fairly large pericenter for Leo I ($r_{\rm peri} \gtrsim 60$ kpc; Sohn et al. 2012) and a low-eccentricity orbit with a similarly great pericenter for the dSph Fornax (e.g., Piatek et al. 2007). Our results suggest that the origin of these dSphs can be accommodated within tidal stirring. Indeed, rotationally supported dwarfs on low-eccentricity and/or large-pericenter orbits may be transformed into dSph-type objects, provided that their DM halos possess shallow density profiles (Table 2). In fact, assuming core-like DM distributions ($\gamma = 0.2$) and small $r_{\rm peri}$, even a single pericentric passage can induce transformation into a dSph. We note that according to recent studies, Leo I has passed through pericenter once (Sohn et al. 2012) and the same conclusion may also apply to Cetus and Tucana (Teyssier et al. 2012).

Lastly, our simulations indicate that none of the $\gamma = 1$ disky dwarfs are disrupted by the host tidal field; of these, only systems on high-eccentricity ($r_{\rm apo}/r_{\rm peri} \gtrsim 5$) and small-pericenter ($r_{\rm peri} \lesssim 25$ kpc) orbits are transformed into dSphs. Interestingly, when $\gamma < 1$, the dSph-like systems that survive are generally on orbits with lower eccentricities and/or larger pericenters compared to those of typical CDM satellites (e.g., Diemand et al. 2007). This finding provides a natural explanation for the rather peculiar orbits of several classic LG dSphs such as Fornax, Leo I, Tucana, and Cetus.

We acknowledge stimulating discussions with Giuseppina Battaglia, Jonathan Bird, Simone Callegari, and Alan McConnachie. This work was partially supported by the Polish National Science Centre under grant NN203580940. The numerical simulations were performed at the Ohio Supercomputer Center (http://www.osc.edu).

REFERENCES

Caputo, F., Cassisi, S., Castellani, M., Marconi, G., & Santolamazza, P. 1999, AJ, 117, 2199
Diemand, J., Kuhlen, M., & Madau, P. 2007, ApJ, 667, 859
D'Onghia, E., Besla, G., Cox, T. J., & Hernquist, L. 2009, Natur, 460, 605
Einasto, J., Saar, E., Kaasik, A., & Chernin, A. D. 1974, Natur, 252, 111
Faber, S. M., & Lin, D. N. C. 1983, ApJL, 266, L17
Fraternali, F., Tolstoy, E., Irwin, M. J., & Cole, A. A. 2009, A&A, 499, 121
Gnedin, O. Y., & Ostriker, J. P. 1999, ApJ, 513, 626
Governato, F., Brook, C., Mayer, L., et al. 2010, Natur, 463, 203
Grcevich, J., & Putman, M. E. 2009, ApJ, 696, 385
Ho, N., Geha, M., Munoz, R. R., et al. 2012, ApJ, 758, 124
Kazantzidis, S., Łokas, E. L., Callegari, S., Mayer, L., & Moustakas, L. A. 2011a, ApJ, 726, 98
Kazantzidis, S., Łokas, E. L., Mayer, L., Knebe, A., & Klimentowski, J. 2011b, ApJL, 740, L24
Kazantzidis, S., Magorrian, J., & Moore, B. 2004a, ApJ, 601, 37
Kazantzidis, S., Mayer, L., Mastropietro, C., et al. 2004b, ApJ, 608, 663
Klimentowski, J., Łokas, E. L., Kazantzidis, S., Mayer, L., & Mamon, G. A. 2009, MNRAS, 397, 2015
Klimentowski, J., Łokas, E. L., Knebe, A., et al. 2010, MNRAS, 402, 1899
Klypin, A., Kravtsov, A. V., Valenzuela, O., & Prada, F. 1999, ApJ, 522, 82
Kravtsov, A. 2010, AdAst, 2010, 1
Kravtsov, A. V., Gnedin, O. Y., & Klypin, A. A. 2004, ApJ, 609, 482
Lewis, G. F., Ibata, R. A., Chapman, S. C., et al. 2007, MNRAS, 375, 1364
Łokas, E. L. 2002, MNRAS, 333, 697
Łokas, E. L., Kazantzidis, S., & Mayer, L. 2011, ApJ, 739, 46
Łokas, E. L., Kazantzidis, S., & Mayer, L. 2012, ApJL, 751, L15
Macciò, A. V., Kang, X., Fontanot, F., et al. 2010, MNRAS, 402, 1995
Mateo, M. L. 1998, ARA&A, 36, 435
Mayer, L., Governato, F., Colpi, M., et al. 2001, ApJ, 559, 754
Mayer, L., Kazantzidis, S., Mastropietro, C., & Wadsley, J. 2007, Natur, 445, 738
Mayer, L., Mastropietro, C., Wadsley, J., Stadel, J., & Moore, B. 2006, MNRAS, 369, 1021
Mayer, L., & Wadsley, J. 2004, MNRAS, 347, 277
McConnachie, A. W. 2012, AJ, 144, 4
McConnachie, A. W., Irwin, M. J., Ferguson, A. M. N., et al. 2005, MNRAS, 356, 979
Mo, H. J., Mao, S., & White, S. D. M. 1998, MNRAS, 295, 319
Moore, B., Ghigna, S., Governato, F., et al. 1999, ApJL, 524, L19
Navarro, J. F., Frenk, C. S., & White, S. D. M. 1996, ApJ, 462, 563
Oh, S.-H., de Blok, W. J. G., Brinks, E., Walter, F., & Kennicutt, R. C., Jr. 2011, AJ, 141, 193
Peñarrubia, J., Benson, A. J., Walker, M. G., et al. 2010, MNRAS, 406, 1290
Piatek, S., Pryor, C., Bristow, P., et al. 2007, AJ, 133, 818
Pontzen, A., & Governato, F. 2012, MNRAS, 421, 3464
Read, J. I., Wilkinson, M. I., Evans, N. W., Gilmore, G., & Kleyna, J. T. 2006, MNRAS, 366, 429
Saviane, I., Held, E. V., & Piotto, G. 1996, A&A, 315, 40
Sohn, S. T., Besla, G., van der Marel, R. P., et al. 2012, ApJ, submitted (arXiv:1210.6039)
Stadel, J. G. 2001, PhD thesis, Univ. Washington
Teyssier, M., Johnston, K. V., & Kuhlen, M. 2012, MNRAS, 426, 1808
Tolstoy, E., Hill, V., & Tosi, M. 2009, ARA&A, 47, 371
Weldrake, D. T. F., de Blok, W. J. G., & Walter, F. 2003, MNRAS, 340, 12
Widrow, L. M., Pym, B., & Dubinski, J. 2008, ApJ, 679, 1239
Yozin, C., & Bekki, K. 2012, ApJL, 756, L18